International Journal Of Industrial Electronics Control and Optimization
Print ISSN: 3517-2645
Online ISSN: 3568-2645
Homepage: https://ieco.usb.ac.ir/

Reliability-based Probabilistic Wind Power Planning Considering Correlation of Load and Wind

Morteza Jadidoleslam | Morteza Ghaseminezhad

Department of Electrical Engineering, Sirjan University of Technology, Sirjan, Iran.[1,2]
Corresponding author's email: jadidoleslam@sirjantech.ac.ir

Article Info

Article type:
Research Article

Article history:
Received: 06 Feb 2022
Received in revised form: 11 Sep 2022
Accepted: 15 Sep 2022
Published online: 21 Nov 2022

Keywords:
Power system reliability
Shuffled frog leaping algorithm
Uncertainty modeling
Wind power planning

ABSTRACT

Wind power has been considered a future alternative to fossil energy resources. However, due to its stochastic nature, the integration of wind power plants (WPPs) into power systems poses some reliability problems such as a mismatch between load profile and efficient wind power generation. This issue can be alleviated by considering the correlation between hourly load and wind speed variations in the planning phase. To this end, a reliability-based wind power planning procedure is proposed and formulated as a stochastic programming problem. The objective function is the minimization of total costs, including capital investment, operating and maintenance, and customer energy not served costs. A new hybrid method that combines features of the load-duration curve and the K-means clustering algorithm is proposed to model the uncertainty of the input data. A shuffled frog-leaping algorithm is used to solve the proposed model. The simulation results indicate that the amount of adaptation between hours with high loads and those with high wind speeds markedly affects the selection of wind sites as optimal locations for WPP installation. Considering this issue can also improve power system reliability in the presence of WPPs.

NOMENCLATURE

$C_{inv}^{\max}$	Budget for investment in wind capacity
$X_{k,s}$	Capacity of the WTG type *k* at wind site *s*
CRF_k	Capital recovery factor of the *k*th WTG type
V_{ci} / V_{co}	Cut-in/cut-out speed of WTG
dr	Discount rate
L_k	Economic life of the *k*th WTG
$EENS_d$	Expected energy not served in block *d*
$\gamma_{d,l}$	Final operating scenario related to cluster *l* in block *d*
$IEAR$	Interrupted energy assessment rate
$IL_{d,l}$	Interrupted load in cluster *l* and block *d*
C_k^{inv}	Investment cost of the *k*th WTG type
$p_{d,l,i}^D$	Load value of the *i*th member in cluster *l* and block *d*
$X_s^{\min}$ / $X_s^{\max}$	Minimum/maximum capacity of wind farm *s*
$N_{d,l}^{HD}$	Number of demand hours of cluster *l* in block *d*
Nh_d	Number of hours in load block *d*
$N_{d,l,s}^{HW}$	Number of wind speed hours at site *s* in cluster *l* and block *d*
$C_k^{O\&M}$	Operating costs of the *k*th WTG type
V_r / P_r	Rated speed/power of WTG
Ω_b	Set of load blocks
Ω_S	Set of wind sites
Ω_K	Set of WTG types
Ω_d	Set of clusters in load block *d*
Ω_{ld}	Set of load data in cluster *l* and block *d*
Ω_{sld}	Set of wind speed data at site *s* in cluster *l* and block *d*
X_T^{wind}	Total installation wind capacity
$WS_{d,l,s,j}$	Wind speed value at site *s* for member *j* of cluster *l* in block *d*
$P_{d,l,s}^{w}$	Wind power at site s for cluster *l* in block *d*
$W_{d,l}$	Weight of cluster *l* in load block *d*
$WS_{d,l}$	Wind speed of cluster *l* in block *d*

DOI: 10.22111/IECO.2022.41721.1416

I. Introduction

The share of renewable resources in the generation sector of many countries is rapidly increasing. Wind power has attracted more attention among different renewable resources because of its specifications, such as very low operating and maintenance costs and the lack of environmental pollution [1, 2]. Due to the random nature of wind speed, the amount of generated wind power is uncertain. In a wind turbine generator (WTG), design parameters, including the turbine rated, cut-in, and cut-out speeds, and the rated capacity are involved in the output power at a specific wind site. Moreover, each WTG has its specific economic and reliability parameters. Hence, identifying the optimal type, number, and location of WTGs is essential to achieving the maximum economic and reliability benefits in wind power planning studies.

On the other hand, there is uncertainty in the forecasted electric demand which affects power system reliability and changes the planning decisions. The reliability of the power system is a key issue in planning studies, especially in the presence of variable resources, such as wind power. In recent years, different papers have analyzed the reliability of power systems in the presence of WPPs using different techniques. For example, in [3], an analytical multi-state model is presented for the adequacy assessments of the generating system incorporating wind power. A procedure is presented in [4] based on the Markov process to model wind farms for reliability evaluation purposes. For a long-term assessment of wind power, an analytical approach is introduced in [5] and used to assess the performance of a hybrid renewable power system. A method to assess the reliability indices is proposed in [6] from the viewpoint of reactive power management for a power system including wind power. A framework for optimal selection of wind turbines is presented in [7], considering the capacity factor of WTG and the EENS reliability index. The proposed method helps compare the performance of wind turbines, but the uncertainties associated with the input data are not considered.

Many papers have analyzed the generation capacity investment problem. In most of them, the problem is solved for conventional generation sources [8, 9]. Nevertheless, because of the uncertain character of wind speed, the WPPs need different models from the conventional plants. In [10], considering both long- and short-term uncertainties of wind power, a two-stage generation expansion planning model is developed, and an ARMA model is adopted to deal with the uncertainties. In [11], the impact of wind energy penetration on the capacity investment and incentives of individual wind power investors is analyzed in the power market. A risk-constrained multi-stage stochastic programming model is proposed in [12] to make optimal decisions for investment in wind capacity.

Some studies have investigated the optimal design of hybrid energy systems including WPPs. In [13], a framework is presented for the optimal design of a grid-connected wind/photovoltaic/storage energy system, and reliability is considered as constraint. For optimal sizing of the components of a hybrid wind/photovoltaic/battery system, an ant lion optimization method is proposed in [14]. The objective function is the minimization of the system's total cost. An approach based on the tunicate swarm optimization method is introduced in [15] to design a wind/photovoltaic/fuel cell hybrid system considering reliability and cost. In these studies, the advantages of hybrid energy systems have been exploited to supply the load, but the effect of uncertainty and the correlation of input data has not been considered in the results.

The commonly used method to deal with uncertainties is stochastic programming [2, 12, 16, 17]. In this approach, which is also used here, uncertainty is represented via scenarios utilizing the input data. A significant aspect of scenario modeling in wind power planning studies is the consideration of the statistical correlation between electric load and wind power generation. Low values of electricity demand usually occur during the night when wind speed (wind power generation) is relatively higher [18]. Hence, considering load and wind as independent phenomena may result in non-optimal investment decisions.

In this paper, regarding the uncertainties and correlation between the input data, such as electric load and wind power, a new method is proposed to represent scenarios in the planning procedure. A stochastic-based programming model is presented for wind power capacity planning, considering the costs and reliability of the electric power system. The proposed model is a combinatorial constrained and nonlinear optimization problem that is properly solved by the shuffled frog leaping algorithm. To demonstrate the performance and effectiveness of the proposed approach, it is implemented in two modified power systems, and several case studies are presented. The main contributions of this paper are as follows:

- Proposing a new hybrid method for scenario modeling that combines features of the load-duration curve and the K-means clustering algorithm in a probabilistic planning framework of WPPs
- Considering and assessing the impact of the correlation between input data on the results of wind power planning from a reliability point of view in the power system.

II. Probabilistic WPP Modeling

A. Uncertainty characterization and scenario modeling

Electric load and wind power generation are not statistically independent values in an electric power system. Low values of electricity demand usually correspond to high wind power generation [18]. Therefore, the uncertainty of both parameters should be jointly investigated. For modeling purposes, hourly historical data can be used for load and wind speeds at different wind sites in one or several years in the studied power system. It is assumed that the historical data are sufficiently scaled to take demand growth into account. Each piece of historical data is a set of values, including the electric load and wind speeds at different wind sites, representing an operating scenario. Considering all scenarios (e.g., 8760 for one year) in solving the problem may result in intractability in a realistic power system. Therefore, a proper method should be adopted for reducing the primary data into a tractable data set.

To model the uncertainties of the electric load and wind speed data, a novel hybrid method is presented that combines features of the load-duration curve (LDC) and the K-means clustering algorithm. The main advantage of the proposed method is achieving scenarios that have maximum concordance with the input data while the correlation between them is maintained.

A flowchart of the proposed method for scenario modeling is depicted in Fig. 1. Evidently, the method is initialized with load and wind speed data input. To create initial scenarios, both load and wind speed data in the same time slot are jointly placed in a group to form an operating scenario. Then, the LDC is formed by sorting the load data in descending order. By so doing, the corresponding wind speed data that are in the same group are also moved, and the temporal correlation between them is maintained. Afterward, the load duration curve is divided into N_{LB} load blocks (LBs), and the number of clusters in each LB (N_{Cl}) is also determined.

In the next step, the K-means clustering algorithm starts by determining the number of iterations. The K-means method is an iterative algorithm that attempts to categorize a dataset into K subgroups (clusters) based on similarity [19]. As shown in Fig. 1, the K-Means method operates as follows:

1) Initialize centroids by randomly selecting K data points as the centers of clusters.
2) Calculate distances between data points and all the centroids.
3) Assign each data point to the closest cluster (centroid).
4) Update centroids by taking the average of all data points that belong to each cluster.
5) Repeat Steps 2 to 4 until the centroids no longer change, or the maximum number of iterations is reached.

After the end of the K-means algorithm, to form the final operating scenarios, the values of wind speeds and load related to each cluster are obtained using (1) and (2), respectively.

$$WS_{d,l,s} = \frac{\sum_{j\in\Omega sld} WS_{d,l,s,j}}{N^{HW}_{d,l,s}};\ \forall d,\forall l,\forall s \quad (1)$$

$$P^{D}_{d,l} = \frac{\sum_{i\in\Omega ld} P^{D}_{d,l,i}}{N^{HD}_{d,l}};\ \forall d,\forall l \quad (2)$$

Moreover, the weight of each final cluster is calculated using the following equation:

$$W_{d,l} = \frac{N^{HD}_{d,l}}{\sum_{l\in\Omega_d} N^{HD}_{d,l}} = \frac{N^{HW}_{d,l,s}}{\sum_{l\in\Omega_d} N^{HW}_{d,l,s}};\ \forall d,\forall l \quad (3)$$

Finally, the output of this method is a reduced set of operating scenarios.

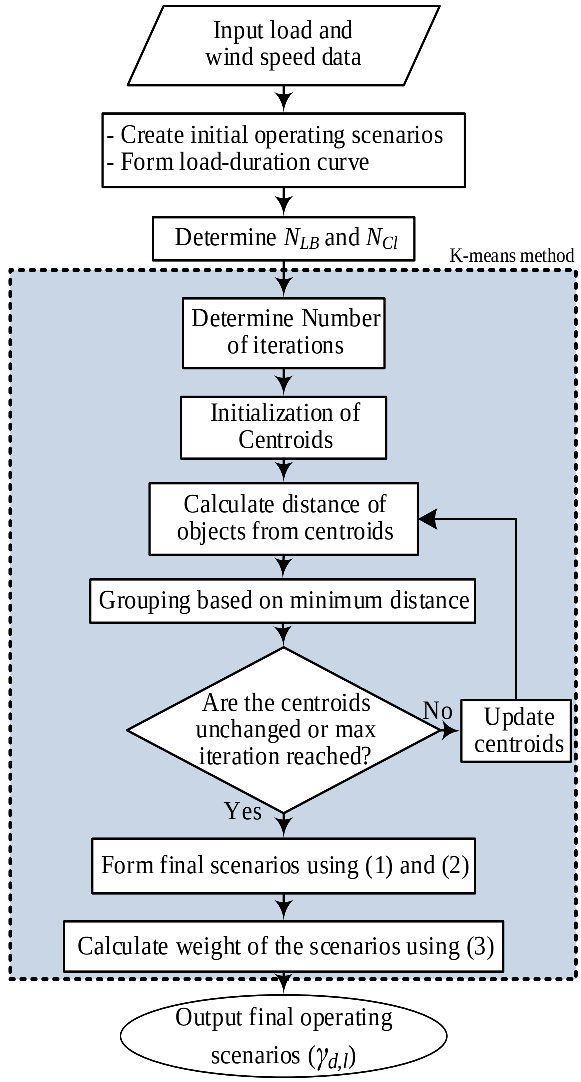

Fig. 1. Flowchart of the proposed method for scenario modelling

Each final scenario contains values of the load, wind speeds at different wind sites, and the occurrence probability that can be expressed as (4).

$$\gamma_{d,l} = \left[P^{D}_{d,l};WS_{d,l,s},\forall s;W_{d,l}\right];\ \forall d,\forall l. \quad (4)$$

B. WPP modeling for reliability evaluation

In addition to an appropriate representation of uncertain input data, two factors should be taken into account for modeling a WPP which directly affect the WTG output. The first one is the relationship between the wind speed and the output power of the WTG, which can be specified using the WTG design parameters, including the rated capacity and the turbine cut-in, cut-out, and rated speeds. The second factor is the unavailability of the WTG, expressed by the WTG forced outage rate (FOR).

Considering the nonlinear relationship between the wind speed and output power of a WTG, the output power curve of a wind turbine can be represented as follows [3, 20].

$$P_{d,l,s}^{WTG} = \begin{cases} P_r(\alpha + \beta \times WS_{d,l,s} + \lambda \times WS_{d,l,s}^2), & V_{ci} \le WS_{d,l,s} \le V_r \\ P_r, & V_r \le WS_{d,l,s} \le V_{co} \\ 0, & \text{otherwise} \end{cases} ;\forall d, \forall l, \forall s. \quad (5)$$

Constants α, β, and λ are calculated using the following equations:

$$\alpha = \frac{1}{(V_{ci} - V_r)^2}\left[V_{ci}(V_{ci} + V_r) - 4(V_{ci}.V_r)\left(\frac{V_{ci} + V_r}{2V_r}\right)^3\right] \quad (6)$$

$$\beta = \frac{1}{(V_{ci} - V_r)^2}\left[4(V_{ci} + V_r)\left(\frac{V_{ci} + V_r}{2V_r}\right)^3 - (3V_{ci} + V_r)\right] \quad (7)$$

$$\lambda = \frac{1}{(V_{ci} - V_r)^2}\left[2 - 4\left(\frac{V_{ci} + V_r}{2V_r}\right)^3\right]. \quad (8)$$

After determining the output power generated by a WTG, the next step is the identification of the WPP model. An analytical method is adopted to build a WPP model that incorporates the FOR of WTG units [3]. In this method, a WPP is divided into two basic parts: wind conditions and WTG units. If WPP comprises identical WTG units with zero FOR, the WPP model will be the same as a single WTG unit. However, if the FOR of WTG units is not zero, wind conditions and the WTG units form a series system (Fig. 2). Therefore, the WPP model can be obtained by combining the capacity outage probability table (COPT) of the WTG units and the wind conditions [3]. To create the COPT of a WTG unit (WTG-COPT), the following procedure is followed:

1) The output states of the WTG are defined as segments of the rated power.
2) The total number of times that an output power falls within one of the output states is determined.
3) The probability of each state is calculated by dividing the total number of occurrences for each output state by the total number of data points.

After forming the WTG-COPT, the multi-state model of a WPP, including multiple WTG units, is created using the following steps.

1) The WTG units with specified rated power and FOR are combined to create a COPT using the conventional COPT algorithm [21].

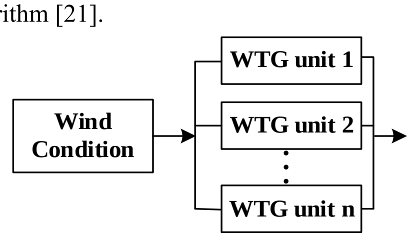

Fig. 2. WPP Model including multiple WTG units.

2) The wind condition model is represented by the WTG-COPT.
3) The wind condition and the COPT of Step 1 are combined to create the multi-state WPP-COPT.

To evaluate the reliability of the generation system, the generation model and load model should be convolved to create the risk model [21]. The generation model (GEN-COPT) is formed using the WPP-COPTs of different WPPs (Table 1) [21]. The first column shows the outage capacity level (O_i) in MW. Thus, the available capacity of the generation system will be the installed capacity minus the outage capacity, which is shown in the second column. In this table, the third column indicates the probability of the generation outage O_i which is calculated using the FOR of the generating units. The load model is described as the LDC displayed in Fig. 3. Based on this figure, for the generation outage of O_i, the load is lost for the period of t_i. Consequently, the loss of load expectation (LOLE) can be calculated as

$$LOLE = \sum_{i=1}^{N} p_i \times t_i. \quad (9)$$

The area under the LDC indicates the energy demand. Hence, the unserved energy due to the generation outage of O_i is E_i, and the expected energy not served (EENS) can be calculated as

$$EENS = \sum_{i=1}^{N} p_i \times E_i. \quad (10)$$

In (9) and (10), N is the number of states of GEN-COPT and p_i is the probability of the generation outage O_i.

III. Problem Formulation

The goal of a power system planner is to identify the optimal wind power investment plans that minimize total costs. Consequently, the objective function of the proposed model is the minimization of total costs, including capital investment, operating and maintenance, and customer energy not served costs. Since the WTGs may have different lifetimes, the annual equivalent cost approach is adopted to evaluate different plans. The proposed wind power planning model is formulated as follows.

TABLE 1
EXAMPLE OF CAPACITY OUTAGE PROBABILITY TABLE.

Capacity outage (MW)	Available capacity (MW)	State probability
O_1	Installed capacity - O_1	p_1
O_2	Installed capacity - O_2	p_2
⋮	⋮	⋮
O_i	Installed capacity - O_i	p_i
⋮	⋮	⋮
O_N	Installed capacity - O_N	p_N

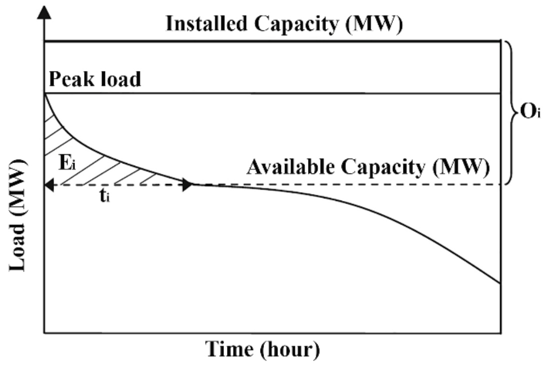

Fig. 3. Load duration curve for reliability evaluation [22].

$$\begin{aligned} \underset{X_{k,s},\forall l,d}{\text{Minimize}} \quad & \sum_{s\in\Omega_S}\sum_{k\in\Omega_K} CRF_k \times C_k^{inv} \times X_{k,s} \\ & + \sum_{s\in\Omega_S}\sum_{k\in\Omega_K} C_k^{O\&M} \times X_{k,s} \\ & + \sum_{d\in\Omega_b} IEAR \times EENS_d \end{aligned} \tag{11}$$

subject to :

$$EENS_d = \sum_{l\in\Omega_d} Nh_d \times W_{d,l} \times IL_{d,l} \; ;\forall d \tag{12}$$

$$X_s^{\min} \le \sum_{k\in\Omega_K} X_{k,s} \le X_s^{\max} \quad ;\forall s \tag{13}$$

$$\sum_{s\in\Omega_S}\sum_{k\in\Omega_K} X_{k,s} = X_T^{wind}. \tag{14}$$

In (11), CRF_k is the capital recovery factor used to calculate the annual equivalent investment cost and is expressed as follows [22]:

$$CRF_k = \frac{dr \times (1+dr)^{L_k}}{(1+dr)^{L_k} - 1}. \tag{15}$$

The objective function of (11) consists of three parts. The first one is related to the capital investment cost of newly installed WPPs. It includes the costs of the turbine, turbine erection, foundations, roads, and grid connections. The second part is the operating and maintenance cost of all WPPs. This cost is calculated annually within the lifetime of a WPP. Finally, the third part is the customer energy not served cost. Reliability and cost models are required to estimate this cost for a power system. Reliability can be assessed by the expected energy not served (EENS) index, using the analytical approach described in Section II. The commonly used cost model to estimate customer energy not served cost is the composite customer damage functions [23]. These functions can estimate a cost factor in ($/MWh), known as the interrupted energy assessment rate (IEAR). Therefore, the cost of energy not served can be calculated using the IEAR factor and EENS index.

In the proposed model, Constraint (12) represents the equation for calculating the EENS reliability index in demand block d. Constraint (13) imposes the limitation of the total wind power installation capacity at a wind site. Wind power capacity, which can be installed at a wind site, is generally limited by factors such as the limitation of a geographical area and wind power availability. Constraint (14) indicates the total targeted wind power capacity that must be constructed in a power system. It is either determined by the future energy plans or forced by the accepted renewable portfolio standard (RPS) mandates. In some cases, Constraint (14) can be replaced by the investment budget constraint as follows:

$$\sum_{s\in\Omega_S}\sum_{k\in\Omega_K} X_{k,s} \le C_{inv}^{\max} . \tag{16}$$

IV. Solution Approach Using the Shuffled Frog Leaping Algorithm

The shuffled frog leaping algorithm (SFLA) is a population-based meta-heuristic optimization method presented in 2003 by Eusuff and Lansey [24]. SFLA is inspired by the evolution of food-seeking frogs. It has a local search ability which makes it a powerful and efficient algorithm. SFLA has been used to solve various problems in power system studies and has shown good efficiency and performance in solving nonlinear and complex optimization problems [2, 9, 25].

In the first step, to start the algorithm, an initial population of 'N' hypothetical frogs is created in the search space. Then, each member of the population is evaluated based on its location (Z_n) using the objective function of the problem, and the population of frogs is sorted in descending order according to their fitness values.

The next step is called local search, which commences by dividing the frogs into a pre-determined number of groups (m). Each group is called a memeplex, and the number of frogs in each one is equal to N/m. In the local search procedure, using the frog leaping rule (Equations 17 and 18), the location of the worst frog (Z_w) changes regarding the best frog (Z_b). This jump is limited by the CP^{max} value.

$$Z_w^{new} = Z_w + CP \tag{17}$$

$$CP = a \times (Z_b - Z_w), \; \|CP\| < CP^{\max} \tag{18}$$

In (17), a is a random number between 0 and 1. If this jump leads to a better position, it will replace the worst frog; otherwise, by substituting the best frog with the global best frog (Z_g), the leaping rule will apply again. After this, if no improvement is achieved, the worst frog will be replaced by a new randomly generated one. The position of the frogs improves by continuing the evolutionary process in the memeplexes for a specified number of iterations.

In the final step, by using the so-called shuffling process, all the frogs are combined and sorted again. The local search and shuffling processes continue until the convergence criterion is met. A flowchart of the implementation of the proposed SFLA method is depicted in Fig. 4. More information and details can be obtained from [24].

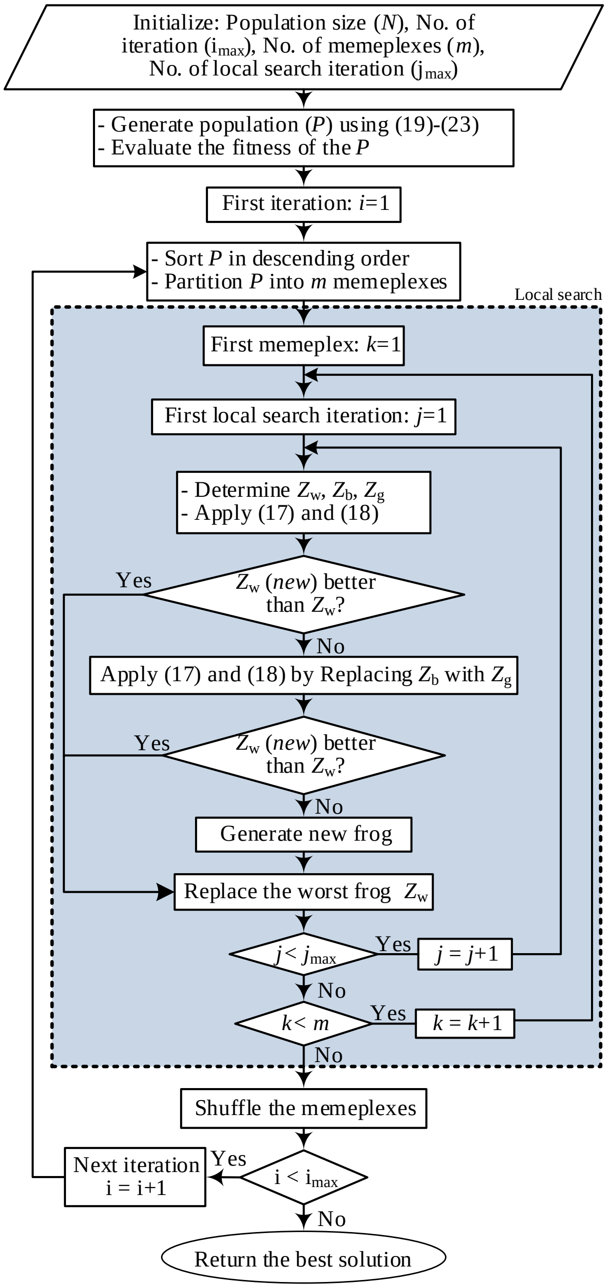

Fig. 4. Flowchart of the SFLA method

It is relatively difficult to apply equality constraints in the SFLA method. An adjustment technique is adopted here to meet Constraints (13) and (14) as follows:

1) Allocate the minimum wind power capacity (X_s^{min}) to each wind site ($s=1,2,\dots,ns$), and calculate the remaining capacity (X_T^R) using (19).

$$X_T^R = X_T^{wind} - \sum_{s\in\Omega_s} X_s^{\min} \tag{19}$$

2) Using the X_T^R, the allocated capacity at the sth wind site (X_s^A) is determined as follows:

$$X_s^A = X_s^{\min} + \text{rand}\left[\max\left(0, X_s^R - \sum_{m=s+1}^{n_s}(X_m^{\max} - X_m^{\min})\right), \left(X_s^{\max} - X_s^{\min}\right)\right] \tag{20}$$

where X_S^R is the remaining capacity after capacity allocation to the *(s-1)*th wind site and calculated using (21).

$$X_s^R = X_T^R - \sum_{m=1}^{s-1} X_m^A. \tag{21}$$

If X_s^A is greater than X_S^R, then $X_s^A = X_S^R$ and the allocated capacity at the remaining wind sites ($s+1,\dots,ns$) will be X_s^{min}.

For the last wind site ($s=ns$), the allocated capacity is given by

$$X_{n_s}^A = X_s^{\min} + (X_T^R - \sum_{s\in\Omega_s\setminus\{n_s\}} X_s^A). \tag{22}$$

Note that the order of wind sites for capacity allocation is randomly chosen. Thus, all wind sites will have the same chance for capacity allocation in the optimization process.

3) Calculate the number of the kth-type WTG units at wind site s using (23).

$$N_{s,k} = \left[\frac{X_s^A}{X_{k,s}}\right] \tag{23}$$

where [ ] is an integer truncation function.

When using the integer truncation function, the total capacity allocated to all wind sites might become less than X_T^{wind}. Hence, to meet Constraint (14) as accurately as possible, the number of the WTG with the lowest rated capacity is adjusted.

V. Numerical Results

To illustrate the performance and effectiveness of the proposed approach, results of different cases based on the RBTS [26] and IEEE-RTS [27] test systems are provided here.

A. Data and parameters

Suppose that four wind sites are considered to develop WPPs in the test systems. The wind speed data are from wind sites at Borujen, Moghar, Moorche-Khort, and Varzane in Isfahan Province, Iran [28]. The mean wind speeds of these sites are 13.5, 15.9, 16.9, and 17.1, respectively. The load data of the RTS [27] are used in the studies. To perform wind power planning, 12 WTG types with different design and operating parameters are considered (Table 2). The FOR and lifetimes of all WTG units are assumed to be 4% and 25 years, respectively. A discount rate of 8% is assumed in the studies. An average IEAR factor of 6.3 K$/MWh is assumed to calculate the energy not served cost [23].

The proper selection of parameters for optimization algorithms has a significant effect on convergence speed and the results obtained. In this paper, the parameters of the employed algorithms (SFLA, PSO, and GA) are selected experimentally by performing several experiments. For this purpose, the SFLA has been run many times using different parameter values. Following that, the appropriate parameters of the algorithm have been selected. To make a fair comparison between all employed algorithms, the parameters of the PSO and GA, such as the initial population and the number of iterations, have been selected proportionally. The selected parameters of the SFLA for both test systems are presented in Table 3.

B. Number of scenarios selected

In the proposed hybrid method for data modeling, the number of final scenarios is determined using the product of the number of LBs (N_{LB}) and the number of clusters in each LB (N_{Cl}). By increasing N_{LB} and N_{Cl}, both modeling accuracy and computational volume increase. To select the proper number of N_{LB} and N_{Cl}, a trade-off must be made between accuracy and computational volume.

To represent load data appropriately, the width of the LBs (in terms of hour span) varies according to the variations (slope) in the LDC curve. For example, since the peak load can greatly affect planning decisions, for the first LB representing the peak load, the width is considered narrower.

Since the number of scenarios affects the accuracy of LOLE index calculation, to find an appropriate number of scenarios, the LOLE is calculated for different numbers of scenarios. For this purpose, the IEEE-RTS test system is considered, and it is assumed that WPPs can be installed at four wind sites with various capacities. The results are depicted in Fig. 5. Evidently, the LOLE is relatively constant after 48 scenarios for all wind power capacities. The results indicate that modeling the operating conditions using 48 scenarios is adequate for generation system reliability assessment and planning studies. These scenario data are provided in Table 4.

TABLE 2
CANDIDATE WTG UNIT PARAMETERS

Type	Rated capacity (MW)	Capital cost (k$/MW)	O&M costs ($/MW-yr)	Rated speed (km/h)	Cut-in speed (km/h)	Cut-out speed (km/h)
W1	0.5	1350	36	40	10	80
W2	0.5	1350	36	45	10	70
W3	1	1250	35	40	12	80
W4	2	1120	30	30	12	55
W5	1	1220	33	33	13	60
W6	1	1250	32	40	14	90
W7	2	1100	35	33	15	50
W8	2	1100	30.5	33	15	60
W9	1	1200	32	37	15	70
W10	1	1250	32	48	18	70
W11	2	1100	30	45	18	70
W12	2	1100	30	35	18	75

TABLE 3
SFLA PARAMETERS

Parameters	RBTS	IEEE-RTS
No. of memeplexes (m)	4	6
CP^{max}	Inf.	Inf.
Population size (N)	40	60
No. of iterations	60	100
Local search iterations	10	10

TABLE 4
LOAD AND WIND SPEED SCENARIOS

#	block	Hours	Load (pu)	Wind speed (pu)			
				Borujen	Moghar	Moorche-khort	Varzane
1	1	81	0.885	0.156	0.268	0.160	0.347
2		66	0.886	0.296	0.095	0.305	0.199
3		61	0.884	0.273	0.126	0.562	0.232
4		55	0.871	0.333	0.335	0.211	0.14
5		85	0.891	0.281	0.135	0.274	0.461
6		52	0.878	0.170	0.130	0.159	0.095
7	2	153	0.812	0.233	0.201	0.479	0.131
8		175	0.812	0.291	0.160	0.373	0.449
9		88	0.817	0.506	0.504	0.519	0.119
10		223	0.803	0.108	0.197	0.147	0.106
11		194	0.818	0.396	0.171	0.196	0.134
12		167	0.822	0.157	0.262	0.169	0.400
13	3	139	0.745	0.389	0.449	0.222	0.138
14		135	0.735	0.327	0.123	0.560	0.244
15		189	0.737	0.155	0.187	0.283	0.454
16		175	0.739	0.184	0.219	0.337	0.129
17		291	0.743	0.078	0.16	0.132	0.129
18		171	0.737	0.45	0.164	0.214	0.123
19	4	185	0.666	0.473	0.215	0.198	0.114
20		372	0.664	0.070	0.208	0.145	0.109
21		270	0.667	0.199	0.101	0.263	0.151
22		215	0.667	0.312	0.146	0.565	0.174
23		202	0.674	0.259	0.391	0.332	0.205
24		256	0.669	0.161	0.199	0.251	0.437
25	5	179	0.608	0.232	0.419	0.239	0.179
26		204	0.602	0.211	0.183	0.549	0.164
27		308	0.600	0.076	0.207	0.118	0.108
28		323	0.593	0.092	0.115	0.251	0.153
29		261	0.591	0.112	0.198	0.214	0.413
30		225	0.608	0.415	0.135	0.225	0.138
31	6	217	0.508	0.381	0.175	0.323	0.214
32		331	0.516	0.086	0.145	0.241	0.347
33		373	0.509	0.083	0.115	0.191	0.112
34		101	0.513	0.255	0.554	0.336	0.143
35		283	0.510	0.078	0.301	0.156	0.171
36		195	0.518	0.101	0.177	0.512	0.184
37	7	234	0.447	0.067	0.116	0.29	0.107
38		185	0.45	0.08	0.141	0.143	0.157
39		177	0.446	0.077	0.35	0.179	0.185
40		116	0.452	0.394	0.131	0.207	0.134
41		97	0.441	0.097	0.153	0.558	0.202
42		191	0.442	0.087	0.169	0.243	0.394
43	8	125	0.375	0.075	0.136	0.324	0.305
44		69	0.384	0.073	0.176	0.526	0.172
45		65	0.384	0.481	0.215	0.240	0.202
46		109	0.386	0.074	0.182	0.188	0.425
47		215	0.377	0.061	0.090	0.251	0.08
48		177	0.389	0.073	0.226	0.181	0.156

C. RBTS case study

The RBTS is a 6-bus test system composed of 11 conventional power plants and five load points. The system peak load and the installed capacity are 185 MW and 240 MW, respectively. Two potential wind sites with the wind regimes of Borujen and Moghar are considered to add WPPs to the RBTS. Three case studies are assumed to demonstrate the performance and effectiveness of the proposed approach. In Case 1, as the base case, the total limitation of wind power capacity is 40 MW. The maximum and minimum capacity constraints at every wind site are 40 and 10 MW, respectively.

Case 2 is similar to Case 1, except that the objective function is replaced by the consumer energy not served cost. In Case 3, the peak load is increased from 185 MW in Case 1 to 200 MW.

The best value of the objective function for Case 1, obtained by the SFLA, is provided in Table 5. For comparison and verification, particle swarm optimization (PSO) and genetic algorithm (GA) are also applied to solve the problem, and the results are listed in this table. The SFLA has found a better solution with a lower cost than the others. The optimal solution is provided in Table 6. Table 7 also shows the values of different components of the objective function and reliability indices for the optimal solution.

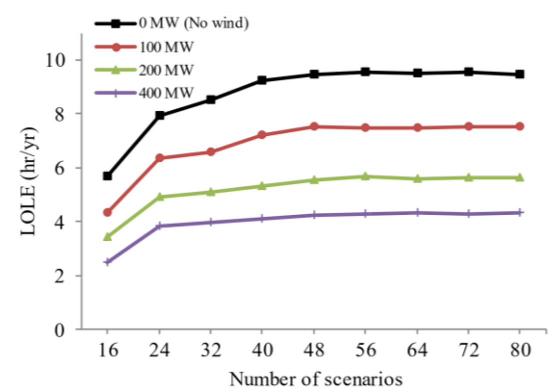

Fig. 5. LOLE values in IEEE-RTS for different numbers of scenarios.

TABLE 5
BEST RESULT VALUES FOR DIFFERENT ALGORITHMS IN RBTS

Case study	Cost (K$)		
	SFLA	PSO	GA
case 1	5362.82	5364.16	5365.53
case 2	27.45	27.45	30.096
case 3	5515.28	5521.38	5525.88

TABLE 6
OPTIMAL SOLUTIONS OF RBTS IN DIFFERENT CASES

Case study	WTG type (No. of WTGs)	
	Borujen	Moghar
case 1	W12 (11)	W12 (9)
case 2	W4 (11)	W4 (9)
case 3	W8 (15)	W12 (5)

The convergence characteristics of the SFLA, PSO, and GA methods are depicted in Fig. 6. The SFLA has superior performance and converges to a better solution faster than the other algorithms. For a better comparison between the algorithms, the SFLA, PSO, and GA are applied 20 times to solve the problem in Case 1, and the results are graphically depicted in Fig. 7. This figure presents the best, average, and worst values obtained by these methods. The results of the SFLA are better than the others, which proves its superiority in terms of success rate and solution quality.

TABLE 7
COMPONENTS OF THE OBJECTIVE FUNCTION FOR OPTIMAL SOLUTION OF RBTS

Case	Total cost (K$)	Annual Investment cost (K$/yr)	O&M cost (K$/yr)	Energy not Served cost (K$/yr)	LOLE (hr/yr)	EENS (MWh/yr)
1	5362.82	4121.87	1200	40.95	0.810	6.480
2	5424.26	4196.81	1200	27.45	0.467	4.343
3	5515.28	4121.87	1215	178.42	3.198	28.23

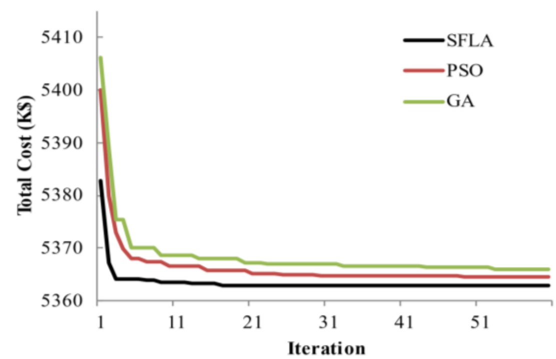

Fig. 6. Convergence characteristics of algorithms in case 1 of RBTS.

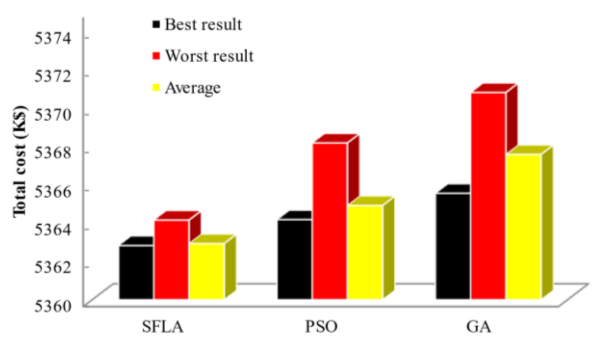

Fig. 7. Best, worst, and average values of algorithms in case 1 of RBTS.

The best values of the objective function in Case 2, obtained by different algorithms, are illustrated in Table 5. In this case, both SFLA and PSO reached the optimal solution, which is provided in Table 6. A comparison of the results for Cases 1 and 2 shows that the optimal plans for these cases significantly differ due to their different objective functions. In case 2, as shown in Table 7, the reliability of the generation system is better than in Case 1. However, the total cost in Case 1 is lower than in Case 2. The results demonstrate the suitability of the proposed approach in searching for different objectives.

Case 3 was introduced to express the effectiveness of the proposed approach in different cases. The results of this case, obtained using various algorithms, are listed in Table 5. The optimal solution obtained by SFLA is better than the other algorithms. This solution is shown in Table 6. In Case 3, the types of the installed WTG units are W8 and W12, whereas in Cases 1 and 2, they are W12 and W4, respectively. The results of this case (Table 7) show that when the peak load of the system is increased, the reliability cost becomes more important in the total cost.

D. IEEE-RTS case study

To express the ability of the proposed approach for solving the problem in a larger-scale power system, it is applied to the RTS system. The RTS is a 24-bus system with 32 conventional generating units. The system peak load and the total generation capacity are 2850 MW and 3450 MW, respectively. All four wind sites are considered to add WPPs to the RTS. Two case studies are examined here. In Case 1, the total WPP capacity limitation is 500 MW. The maximum and minimum capacity constraints at every wind site are 200 and 20 MW, respectively. In Case 2, the customer energy not served cost is considered as the objective function instead of the original one.

The best values of the objective function in both cases, obtained via the SFLA, PSO, and GA methods, are given in Table 8. The results of the SFLA are superior to the others in both case studies. The optimal solutions for these cases are shown in Table 9. Various components of the objective function for these cases are also depicted in Table 10. Because of the different objective functions used in the model, there is a considerable difference between optimal plans and reliability indices. In Case 2, the WTG types for all four wind sites are type W4, whereas in Case 1, they are W4, W8, and W12.

TABLE 8
BEST OBJECTIVE FUNCTION VALUES FOR DIFFERENT ALGORITHMS IN RTS

Case study	Cost (K$)		
	SFLA	PSO	GA
case 1	69592.86	69625.14	69648.76
case 2	2218.11	2241.29	2258.26

TABLE 9
OPTIMAL SOLUTIONS OF RTS IN DIFFERENT CASES

Case	WTG type (No. of WTGs)			
	Borujen	Moghar	Moorche-khort	Varzane
1	W4 (81)	W12 (10)	W12 (59)	W8 (100)
2	W4 (87)	W4 (10)	W4 (53)	W4 (100)

Fig. 8 displays the convergence characteristics for the different optimization algorithms. The SFLA converges to a better solution with a high convergence speed. Results of Case 1, obtained from 20 independent runs using different algorithms, are illustrated in Fig. 9. The best, average, and worst results of the SFLA are better than those of other algorithms. In RTS, the performance of SFLA is more evident where the number of decision variables is increased compared to the RBTS system.

TABLE 10
COMPONENTS OF THE OBJECTIVE FUNCTION FOR OPTIMAL SOLUTIONS OF RTS

Case	Total cost (K$)	Annual Investment Cost (K$/yr)	O&M cost (K$/yr)	Energy not served cost (K$/yr)	LOLE (hr/yr)	EENS (MWh /yr)
1	69592.86	51826.84	15100	2666.01	3.80	423.18
2	69678.22	52460.11	15000	2218.11	3.25	352.08

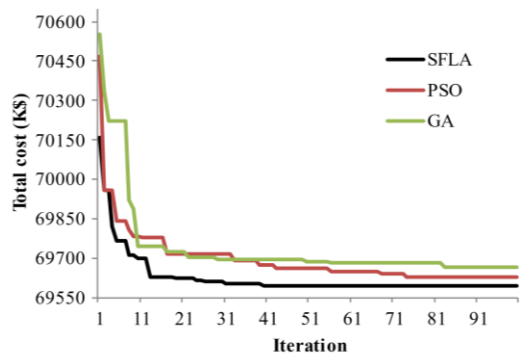

Fig. 8. Convergence characteristics of algorithms in case 1 of RTS.

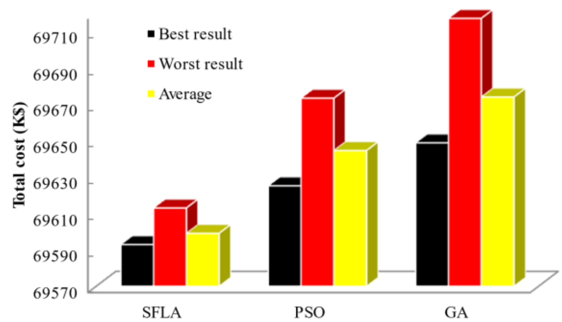

Fig. 9. Best, worst, and average values of algorithms in case 1 of RTS.

E. Considering the correlation between input data

To demonstrate the impact of considering the correlation between input data on the optimal planning schemes, the installed capacity of WPPs for RBTS and RTS is depicted in Figs. 10 and 11, respectively. Based on Fig. 10, although the average wind speed in Borujen is lower than Moghar, more capacity of WPP is installed in the Borujen wind site. This is due to the greater adaptation between hours with high electricity demand and high wind speed in Borujen compared with Moghar. Similar results can be observed in Fig. 11, where the results of RTS are shown. Because of the suitable adaptation between the load and wind speed in Borujen, the installed capacity is more than Moghar and Moorche-Khort which have a higher average wind speed than Borujen. These results demonstrate the importance of considering the correlation between the input data in wind power planning studies.

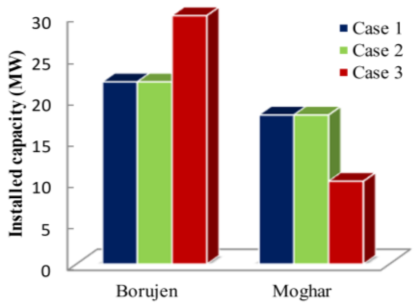

Fig. 10. Installed capacity of WPPs in RBTS system.

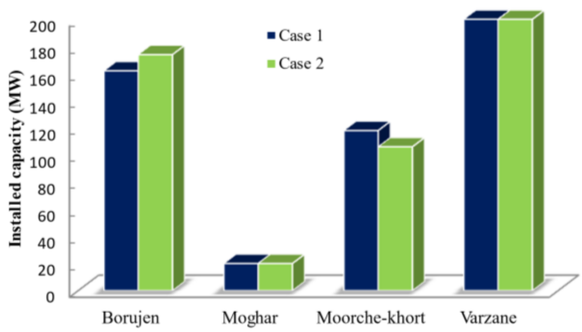

Fig. 11. Installed capacity of WPPs in RTS system.

F. Sensitivity analysis

Herein, the effect of wind speed variations on the planning results is analyzed. To this end, wind power planning is carried out while neglecting wind power uncertainty in the RBTS test system (Case I). The results are compared with the results of considering wind power uncertainty (Case II). In both cases, the peak load is 185 MW, and the objective function is energy not served cost. It is assumed that the wind speed at the wind sites varies from -10% to +10% of the original values. The LOLE reliability index for both cases is depicted in Fig. 12. Case II is more robust than Case I. Especially when the wind speed is reduced, there is a significant increase in the LOLE index in Case I and, consequently, the cost of unsupplied energy. Furthermore, with increasing the wind speed, there is a slight improvement in the LOLE index for this case. Accordingly, the proposed approach for wind power planning considering the uncertainties is more flexible and robust, which can help the planner reduce the costs and system risks.

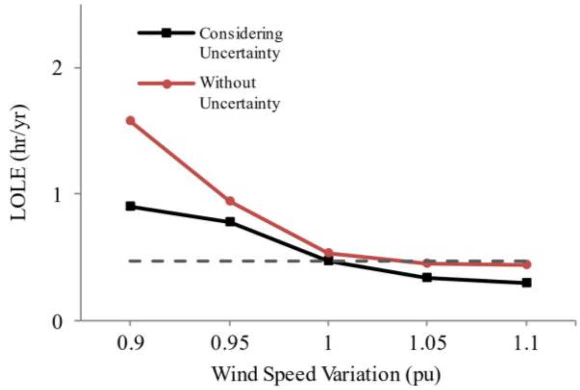

Fig. 12. LOLE index versus wind speed variations.

VI. Conclusion

This paper presents an approach for identifying optimal wind power investment plans, considering the uncertainty and correlation of electric load and wind power. The SFLA method is successfully applied to solving the proposed model. Based on the results of different case studies, the following conclusions can be drawn: 1) Statistical correlations between electric load and wind speeds significantly affect the optimal WPP investment plans. Thus, considering load and wind speeds as independent phenomena may result in non-optimal decisions. 2) A high average wind speed at a specific wind site is not sufficient for the better reliability performance of a WPP. The amount of adaptation between hours with high electricity demand and those with high wind speed also plays a key role in this regard. 3) When reliability receives more attention, the impact of the adaptation between wind and load speeds on the results becomes more salient. 4) Future works should include the development of a model considering the reactive power and transmission lines in the planning procedure.

References

[1] E. Jafari, "Coordinated Operation of Wind Farms, Cascaded Hydro, Photo-voltaic, and Pump-storage Considering WT-ANN-ICA Hybrid Prediction Method," International Journal of Industrial Electronics, Control and Optimization, vol. 4, no. 1, pp. 127-139, 2021.
[2] M. Jadidoleslam, A. Ebrahimi, and M. A. Latify, "Probabilistic transmission expansion planning to maximize the integration of wind power," Renewable Energy, vol. 114, pp. 866-878, 2017.
[3] R. Billinton and Y. Gao, "Multistate Wind Energy Conversion System Models for Adequacy Assessment of Generating Systems Incorporating Wind Energy," IEEE T Energy Conver, vol. 23, pp. 163-170, 2008.
[4] M. Haji-Bashi and A. Ebrahimi, "Markovian Approach Applied to Reliability Modeling of a Wind Farm," Turk J Electr Eng Co, vol. 22, pp. 287-301, 2014.
[5] S. Eryilmaz, İ. Bulanık, and Y. Devrim, "Reliability based modeling of hybrid solar/wind power system for long term performance assessment," Reliability Engineering & System Safety, vol. 209, pp. 1074-78, 2021.
[6] A. Heshmati and H. R. Najafi, "Wind farm incorporation in

reliability assessment of power systems from the viewpoint of reactive power management," Journal of Energy Management and Technology, vol. 4, no. 4, pp. 57-67, 2020.
[7] S. Eryilmaz and J. Navarro, "A decision theoretic framework for reliability-based optimal wind turbine selection," Reliability Engineering & System Safety, vol. 221, p. 108291, 2022.
[8] S. Rebennack, "Generation Expansion Planning under Uncertainty with Emissions Quotas," Electr Pow Syst Res vol. 114, pp. 78-85, 2014.
[9] M. Jadidoleslam and A. Ebrahimi, "Reliability Constrained Generation Expansion Planning by a Modified Shuffled Frog Leaping Algorithm," Electr Pow Energy Syst, vol. 64, pp. 743-751, 2015.
[10] O. H. Abdalla, L. Smieee, M. A. A. Adma, and A. S. Ahmed, "Two-stage robust generation expansion planning considering long- and short-term uncertainties of high share wind energy," Electric Power Systems Research, vol. 189, p. 106618, 2020.
[11] S. Mokhtari and K. K. Yen, "Impact of large-scale wind power penetration on incentive of individual investors, a supply function equilibrium approach," Electric Power Systems Research, vol. 194, p. 107014, 2021.
[12] L. Baringo and A. J. Conejo, "Risk-constrained multi-stage wind power investment," IEEE Trans Power Syst, vol. 28, pp. 401-411, 2013.
[13] A. Naderipour et al., "Optimal design of hybrid grid-connected photovoltaic/wind/battery sustainable energy system improving reliability, cost and emission," Energy, vol. 257, p. 124679, 2022 2022.
[14] S. M. H. Baygi and J. Farzaneh, "Application of Artificial intelligence techniques for optimum design of hybrid grid-independent PV/WT/battery power system," International Journal of Industrial Electronics, Control and Optimization, vol. 3, no. 3, pp. 275-290, 2020.
[15] R. Krishnakumar and C. S. Ravichandran, "Reliability and Cost Minimization of Renewable Power System with Tunicate Swarm Optimization Approach Based on the Design of PV/Wind/FC System," Renewable Energy Focus, vol. 42, pp. 266-276, 2022.
[16] T. Cai, M. Dong, H. Liu, and S. Nojavan, "Integration of hydrogen storage system and wind generation in power systems under demand response program: A novel p-robust stochastic programming," International Journal of Hydrogen Energy, vol. 47, no. 1, pp. 443-458, 2022.
[17] R. Li, S. Guo, Y. Yang, and D. Liu, "Optimal sizing of wind/ concentrated solar plant/ electric heater hybrid renewable energy system based on two-stage stochastic programming," Energy, vol. 209, p. 118472, 2020.
[18] S. Wharton and J. K. Lundquist, "Atmospheric Stability Affects Wind Turbine Power Collection," Environ Res Lett, vol. 7, pp. 1-9, 2012.
[19] R. Xu and D. Wunsch, "Survey of Clustering Algorithms," IEEE Trans Neural Net, vol. 16, pp. 645-678, 2005.
[20] R. Billinton and A. A. Chowdhury, "Incorporation of wind energy conversion systems in conventional generating capacity adequacy assessment," IEE Proc. C vol. 139, pp. 47-56, 1992.
[21] R. Billinton and R. N. Allan, Reliability Evaluation of Power Systems, 2nd ed. Plenum, 1996.
[22] H. Seifi and M. S. Sepasian, Electric Power System Planning: Issues, Algorithms and Solutions. Springer 2011.
[23] R. Billinton and W. Wangdee, "Predicting Bulk Electricity System Reliability Performance Indices Using Sequential Monte Carlo Simulation," IEEE T Power Deliver, vol. 21, pp. 909-917, 2006.
[24] M. M. Eusuff and K. Lansey, "Optimization of Water Distribution Network Design Using the Frog Leaping Algorithm," J Water Res Planning Manage, vol. 129, pp. 21-25, 2003.
[25] M. Wang, Q. Zhang, H. Chen, A. A. Heidari, M. Mafarja, and H. Turabieh, "Evaluation of constraint in photovoltaic cells using ensemble multi-strategy shuffled frog leading algorithms," Energy Conversion and Management, vol. 244, p. 114484, 2021.
[26] R. Billinton et al., "A Reliability Test System for Educational Purposes-Basic Data," IEEE Power Engineering Review, vol. 9, pp. 67-68, 1989.
[27] Reliability Test System Task Force, "The IEEE reliability Test System-1996," IEEE Trans Power Syst, vol. 14, pp. 1010-1020, 1999.
[28] Renewable Energy Organization of Iran. (2016). Wind Energy Office Data. Available: http://www.suna.org

Morteza Jadidoleslam received the B.Sc. degree from the Shahid Bahonar University of Kerman, Kerman, Iran, in 2008, the M.Sc. degree from the Isfahan University of Technology, Isfahan, Iran, in 2011, and the Ph.D. degree from Isfahan University of Technology, Isfahan, Iran, in 2017, all in electrical engineering. He is currently an Assistant Professor in the Department of Electrical Engineering, Sirjan University of Technology, Sirjan, Iran. His research interests are power system planning and operation, renewable energy, and micro grids.

Morteza Ghaseminezhad was born in Bardsir, Iran, in 1985. He received the B.Sc. degree from Electrical Engineering Department of Shahid Bahonar University, Kerman, Iran, in 2007 and the M.Sc. and Ph.D. Degree in electrical engineering from Shahed University, Tehran, Iran, in 2010, and 2017, respectively. At the present, he is the assistant professor of electrical engineering department in Sirjan University of Technology. His especial fields of interest include transient in power systems, power quality and electrical machines.